

WIGNER CRYSTALLIZATION IN THE LOWEST LANDAU LEVEL FOR $\nu \geq 1/5$

V. A. Kashurnikov

Moscow State Engineering Physics Institute, 115409 Moscow, Russia

N. V. Prokof'ev, B. V. Svistunov and I. S. Tupitsyn

Russian Research Center "Kurchatov Institute", Moscow 123182, Russia

By means of exact diagonalization we study the low-energy states of seven electrons in the lowest Landau level which are confined by a cylindric external potential modelling the rest of a macroscopic system and thus controlling the filling factor ν . Wigner crystal is found to be the ground state for filling factors between $\nu = 1/3$ and $\nu = 1/5$ provided electrons interact via the bare Coulomb potential. Even at $\nu = 1/5$ the solid state has lower energy than the Laughlin's one, although the two energies are rather close. We also discuss the role of pseudopotential parameters in the lowest Landau level and demonstrate that the earlier reported gapless state, appearing when the short-range part of the interaction is suppressed, has nothing in common with the Wigner crystallization in pure Coulomb case.

PACS numbers: 73.20.Dx, 73.40.kp

I. INTRODUCTION

After the Laughlin states (LS) were proposed as new ground states of strongly correlated 2D-electron liquid in external magnetic field [1], they were intensively compared to the known ground states (GS), in particular with the Wigner crystal (WC), to understand the conditions and limitations of the experimental observation of the fractional quantum Hall effect (FQHE). In fact, even LS themselves may be called "liquid" only for sufficiently large filling factors $\nu = 1/m$ (for $m \leq m_c \approx 71$ [2]), as follows from the formal analogy between the LS and the two-dimensional one-component plasma at dimensionless temperature $T = 1/2m$. At very small T the equivalent plasma undergoes Kosterlitz-Thouless transition to the state with the finite shear modulus and should be rather viewed as a solid [3].

For the Coulomb system, however, the critical value, m_c , is of academic importance only, since it is easy to prove that in the solid phase the Laughlin state differs qualitatively from the genuine GS. Indeed, in a solid with non-zero shear modulus and Coulomb interaction between the particles the sound dispersion law in magnetic field is $\omega_k \sim k^{3/2}$ [4]. Calculating the mean-square displacement in such a solid at $T = 0$ one finds a convergent answer $\langle (u(0) - u(R \rightarrow \infty))^2 \rangle \sim \int d^2k / \omega_k \rightarrow \text{const}$. On another hand, the equivalence between the LS and the finite-temperature 2D plasma implies divergency of this correlator. [In solid plasma this divergency is due to the transverse-sound dispersion law: $\langle (u(0) - u(R \rightarrow \infty))^2 \rangle \sim T \int d^2k / \omega_k^2 \sim T \ln(R)$]. Thus solid LS maintains the topological order only, which is typical for the 2D solid with short-range interactions in magnetic field when $\omega_k \sim k^2$, in agreement with the fact that LS is a perfect trial function for GS of the system with short-range interactions.

Having established that in the Coulomb system LS provides incorrect GS for large $m > m_c$, one may further suspect that it may give the way to the Wigner crystal at much smaller m . Early variational calculations performed for the electrons at the lowest Landau level and neglecting Landau-level-mixing effects [5] gave strong evidence that WC has lower energy already at $\nu = 1/7$, which explained why there is no Hall conductivity quantisation at this filling factor. Mixing effects, which are very important in real systems, were taken into consideration in Refs. [6]. It was found that virtual transitions between the Landau levels promote WC states and make LS unstable even at $\nu = 1/3$ for sufficiently large mixing parameter $\lambda = \nu^{1/2} (e^2 / \epsilon l_H) / \omega_c$, where $l_H = (1/eB)^{1/2}$ is the magnetic length in the external field B , ϵ is the dielectric constant, and $\omega_c = eB/m^*$ is the cyclotron frequency for electrons with the effective mass m^* . (We use units $\hbar = c = 1$). For the $\lambda = 0$ case the results of Refs. [5,6] predict LS to be the ground state for filling factors $\nu = 1/3$ and $1/5$.

An essential drawback of previous calculations is their variational character. Since the difference in energy (per particle) between the LS and WC is only a few percent in Coulomb units $e^2 / \epsilon l_H$, only filling factors $\nu = 1/m$ with odd m , were the liquid GS is known reasonably well, were analyzed in detail. We simply do not know other liquid states with necessary accuracy to compare them with the variational functions we have at hand for WC. Moreover, it is impossible to use LS energies $E_{LS}(1/m)$ to derive $E_{Liquid}(\nu)$ for other filling factors by extrapolation, because of the cusps that must occur at filling factors where FQHE exists.

It is believed that due to this cusping down at simple rational ν there may arise reentrant WC-LS-WC behaviour around $\nu = 1/5$ (and possibly $\nu = 1/3$). Available experimental data seem to give strong evidence that WC exists at $\nu = 0.21$ [7–9]. However, this conclusion is based entirely on the divergent, activation-type resistivity $\rho_{xx} \rightarrow \infty$ at low temperatures, thus one may not rule out the possibility of explaining the data by impurity induced electron localisation.

The other way to study this problem is by means of exact diagonalization. We are not aware of any systematic attempt to look for the WC states in numerical simulations of FQHE, although in [11] WC was suggested as a possibility to explain peculiar degeneracies in the numerical spectra as a function of inter-particle pseudo-potential. As we show below, the collapse of the LS to the gapless state at $\nu = 1/3$ found in [11], has nothing to do with the transition to WC state. The best numerical calculations were done on a sphere for as many as $N = 12$ particles on 25 orbits [10]. The spherical geometry being perfect for the study of FQHE itself, is practically ineligible for looking at Wigner crystallization. There is little doubt that the optimal electron configuration in the WC is the triangular lattice, which is topologically prohibited on a sphere.

To give further theoretical support to the idea that WC state may be GS of the 2D electron gas at $\nu < 1/5$, we calculated numerically GS and low-lying excited states for the cluster of 7 electrons in the lowest Landau level and in the confining potential. (The number of particles in the system must be 7,12 etc., depending on the sample geometry, to account for the hexagonal symmetry of WC). The confining potential was derived from the Coulomb interaction between an electron in the cluster and electrons outside the "first coordination sphere" (that is at a distance equal or larger than $\sqrt{3}a$, where a is the atomic length in the triangular lattice). In fact, the radius, a , of this confining potential was our main variable determining an effective filling factor ($a \sim \nu^{-1/2}$). It was found that WC state (see below the discussion of what has to be thought of as WC for the system of only 7 particles) is GS of the system for all filling factors between 0.4 and 1/5 except for the region $0.34 > \nu > 0.294$ (including $\nu = 1/3$), where LS was essentially present in the structure of GS. These results strongly suggest (keeping reservations for possible finite-size corrections) that LS at $\nu = 1/3$ is very close in energy to WC, and that in a perfect Coulomb system at $\nu = 1/5$ the ground state may be WC. There is almost no doubt then that WC must exist between these two filling factors.

Our calculation completely ignores impurities and Landau-level-mixing effects, as well as possible screening of the bare Coulomb potential, and the role of electron delocalisation in the direction perpendicular to the 2D plane. Some of these factors are very important in real systems, and, e.g., electron screening, may work in favour of LS. We believe that experimental data of Refs. [7–9], demonstrating FQHE at $\nu = 1/5$, can be accounted for along these lines. We are planning to study different pseudo-potentials in a separate paper.

II. HAMILTONIAN AND NUMERICAL METHOD

We study a 2D system of $N_e = 7$ electrons in the magnetic field in a confining potential. Since we intend to model the macroscopic system in the finite-cluster calculation, we derive this confining potential as resulting from the Coulomb interaction between an electron in the cluster and other electrons outside the "first coordination sphere". The unit length $a(\nu)$ in the WC lattice is expressed through the electron density n_e and filling factor $\nu = 2\pi l_H^2 n_e$ as

$$\frac{\sqrt{3}}{2} a^2 n_e = 1 \quad \text{or} \quad a^2 = \frac{4\pi}{\nu\sqrt{3}}, \quad (2.1)$$

(from now on we measure all distances in units of l_H , which is kept fixed in our calculation). To account for the short-range correlations we place surrounding electrons on the coordination spheres of the WC state. One may better view our system as originating from the classical crystal with atoms sitting on the $m = 0$ orbits $\Psi_j(z_j) = \Psi_{m=0}(z_j - Z_j)$, with the positions Z_j forming an ideal triangular lattice corresponding to the filling factor ν . We then allow for full quantum dynamics of 7 electrons with $Z_j = 0$ and $|Z_j| = a$ while keeping other electrons frozen, but coupled to the first 7 ones by Coulomb forces. Thus obtained confining potential is not spherically symmetric, and may cause transitions changing the momentum of an inner electron by $\Delta m = \pm 6n$. Obviously, this coupling will promote "crystal" state for the central cluster. To avoid this shortcoming we ignore all these transitions, keeping only the diagonal part of the interaction; this procedure is equivalent to rotational averaging of the confining potential.

We also ignore Landau level mixing, which means that Coulomb interaction is the only energy scale in the problem. To simplify the notation we measure all energies in units $e^2/(\epsilon l_H)$. Working in the symmetric gauge $\vec{A} = 1/2H(-y, x)$ we place the electrons on up to 31 orbits corresponding to the angular momentum states ranging from $m = 0$ to $m = 30$. The maximum number of orbits in a given calculation was defined by the condition that occupation numbers $\langle n(m) \rangle$, giving the probability to find an electron in the state with the orbital momentum m , stop changing (at

the level of 0.001), when the number of orbits is increased, and that the largest momentum state be empty with the same accuracy.

The starting Hamiltonian then can be written as

$$H = \sum_{m_1, m_2, m_3, m_4} V_{m_1, m_2, m_3, m_4} a_{m_1}^\dagger a_{m_2}^\dagger a_{m_3} a_{m_4} + \sum_m V_m^{(MF)} a_m^\dagger a_m , \quad (2.2)$$

where a_m^\dagger creates an electron in the state

$$|m\rangle = \frac{z^m}{\sqrt{2\pi 2^m m!}} e^{-|z|^2/4} . \quad (2.3)$$

In the symmetric gauge the interaction matrix elements in the first term in (2.2) satisfy the conservation law $m_1 + m_2 - m_3 - m_4 = 0$ and may be written as

$$V_{m_1, m_2, m_3, m_4} = \frac{(-1)^{m_1+m_3}}{2^M (\prod_{i=1}^4 m_i!)^{1/2}} \sum_{k_1=0}^{\leq m_1, m_4} \sum_{k_2=0}^{\leq m_2, m_3} \times (-2)^{k_1+k_2} k_1! k_2! C_{k_1}^{m_1} C_{k_2}^{m_2} C_{k_1}^{m_3} C_{k_2}^{m_4} I(M, k_1, k_2) , \quad (2.4)$$

$$I(M, k_1, k_2) = \int_0^\infty dq \frac{V_C(q)}{2\pi} q^{2M-2k_1-2k_2+1} e^{-q^2} , \quad (2.5)$$

where $M = m_1 + m_2$, $C_j^i = i!/(j!(i-j)!)$, and $V_C(q)$ gives the Fourier component of the pair potential. For the case of Coulomb interaction $V_C(q) = 2\pi/q$, and the final expression simplifies to

$$V_{m_1, m_2, m_3, m_4} = \frac{(-1)^{m_1+m_3} \sqrt{\pi}}{2^{2M+1} (\prod_{i=1}^4 m_i!)^{1/2}} \sum_{k_1=0}^{\leq m_1, m_4} \sum_{k_2=0}^{\leq m_2, m_3} \times (-4)^{k_1+k_2} [2(M - k_1 - k_2) - 1]!! C_{k_1}^{m_1} C_{k_2}^{m_2} C_{k_1}^{m_3} C_{k_2}^{m_4} . \quad (2.6)$$

To construct the confining potential one has to calculate the diagonal matrix elements for one electron staying on orbit $|m\rangle$ and the other electron staying on orbit $\Psi_{m=0}(z - Z_j)$ (for the diagonal matrix element it does not matter whether the state $\Psi_{m=0}(z - Z_j)$ is defined in the same gauge as states $|m\rangle$ or obtained by gauge transforming the state $|m=0\rangle$). Thus we have

$$V_m^{(MF)} = \sum_{j=2,3,\dots} V_m(Z_j) , \quad (2.7)$$

where the sum is over all coordination spheres starting from the second one, and

$$V_m(Z_j) = (-1)^{m_2-m_1} m! \sum_{k=0}^m \frac{(-1)^k 2^k}{k! [(m-k)!]^2} \int_0^\infty dq \frac{V_C(q)}{2\pi} q^{2m-2k+1} e^{-q^2} J_0(q | Z_j |) . \quad (2.8)$$

Here $J_0(q)$ is the Bessel function. In practice we constructed the confining potential by summing over all coordination spheres inside the radius $100l_H$.

Our diagonalization procedure is arranged as follows. For the calculation of the groundstate level we use the standard modified Lanczos method with the straightforward iteration procedure (see, for example, [12]), while for the calculation of the lowest excited levels we apply more sophisticated method [13]. The set of approximate eigenfunctions is reconstructed from Relay's tridiagonal matrix [14], and the trial wavefunction is expanded in it. As is known, the set inevitably involves a substantial number of spurious states, due to numerical errors. These states, however, may be easily identified by their negligible contribution to the expansion of the trial wavefunction. Upon exclusion of the spurious states the set is subjected to the orthogonalization and correction by Newton method. The relative (with respect to a characteristic interlevel spacing) errors in the energy level calculation are typically of order $10^{-13} \div 10^{-11}$ for the groundstate, and of order $10^{-9} \div 10^{-5}$ for some ten first excited states. Since the Hamiltonian conserves the total angular momentum we take advantage of this symmetry to proceed separately for each angular momentum sector.

III. RESULTS FOR THE LOW-ENERGY STATES

Before presenting our numerical results for the ground and first excited states in the cluster, let us first discuss how one may discriminate between the liquid and solid states in such a small system. The most obvious solution is to look at the pair correlation function. From the symmetry considerations we expect (at least for small filling factors) that one particle will be always staying near the origin, and the rest 6 particles will have their density distribution being peaked at a distance $\approx a(\nu)$ apart. These particles are mutually correlated over the angle θ between their coordinates on the "first coordination sphere". The appropriate pair correlation function thus can be defined as

$$g_\alpha(\theta) = \langle \alpha | \Psi^\dagger(z_1)\Psi^\dagger(z_2)\Psi(z_2)\Psi(z_1) | \alpha \rangle, \quad |z_1| = |z_2| = a, \quad (3.1)$$

where $\theta = \arg(z_1) - \arg(z_2)$ varies in the interval $(0, \pi)$. In the solid state we expect three well-defined oscillations in $g(\theta)$, while in the liquid these oscillations should be strongly damped. It is difficult to predict a priori the amplitudes of oscillations, but it is known (see, e.g., [3]) that pair correlations in the LS disappear very rapidly at $\nu = 1/3$ and $\nu = 1/5$. Our definition of g is not quite standard, but we believe that its qualitative behaviour is the same (we verify this point explicitly below). Anyway, the abrupt change of the ground state correlator $g_G(\theta)$ as a function of ν is indicative of the solid-liquid transition.

One may also expect some qualitative differences in the structure of the low-energy spectra of WC and LS. By construction, our Hamiltonian is cylindrically symmetric and conserves the total angular momentum $M = \sum_m mn(m)$. In the solid phase of the macroscopic system this symmetry is spontaneously broken. For the triangular lattice under study the symmetry is broken by coupling momenta $M_G \pm 6n$ (where M_G is the ground state angular momentum and n is an integer). Thus in the solid phase we expect the states $|M_G \pm 6n\rangle$ to form a subset of the lowest excited states well separated from the rest of the excitation spectrum in these sectors. There is no special reason to have the lowest excitations at $M_G \pm 6n$ in a liquid phase, nor should they have much lower energies than excited states with $M = M_G$.

One remark is in order here. In a really macroscopic solid, the lowest states are those corresponding to the system rotation as a whole, with the energy going as $E \sim (M - M_G)^2/L^4$ where L is the system's size. The crystal symmetry is not present in the structure of the spectrum explicitly, but it is important that the states, mixed by the symmetry breaking fields, are among the lowest ones. In the finite system of only seven particles we do not expect the spectrum to be quadratic in $M - M_G$, since this property in the rotating solid is achieved by creating extra zeros in the wavefunction $\tilde{\Psi}(z_j) = \Psi(z_1, z_2, \dots, z_N)$ for fixed $\{z_1, \dots, z_{j-1}, z_{j+1}, \dots, z_N\}$. This procedure may be too costly in energy in a small system. For $N_e = 7$ rotation is equivalent to the correlated motion of six particles. The first rotating state which requires no extra zeros in $\tilde{\Psi}(z_j)$ is that with $|M - M_G| = 6$.

The other point concerns the consistency of our procedure of controlling the filling factor according to equations (2.1) and (2.8). Since the confining potential is derived from the crystal state, a natural question arises of how good is this approximation for modelling a liquid environment. There is no doubt that at $\nu = 1/3$ the ground state is well described by LS with the ground-state angular momentum $M_G = 3N_e(N_e - 1)/2 = 63$. No matter how trivial, this fact is not at all predetermined by the numerical procedure used. Its validity was confirmed in our calculations, thus demonstrating consistency between Eq. (2.1) and the effective filling factor. Similarly, we observed that $M_G = 5N_e(N_e - 1)/2 = 105$ when $\nu = 0.198$ in Eq. (2.1). The consistency of our "mean-field" procedure follows also from the fact that for all $\nu < 1/2$ the position of the maximum in the particle density $\rho(R)$ coincides with $a(\nu)$.

In Table I we present our data for the ground state angular momentum as a function of filling factor. For $\nu > 0.705$ the system is described by the IQHE state with occupation numbers $n_i = 1$ for $i = 0, 1, \dots, 6$. After drastic transformations in the range of densities between 0.705 and 0.46 GS evolves into the state with well-defined pair correlation function $g(\theta)$. We note, that starting from rather high filling factor 0.587 the angular momentum of the ground state changes by 6. Also, the lowest excited state is always in the sector $M_G \pm 6$.

To identify the nature of GS we present in Fig.1 the plots of $g(\theta)$ calculated for critical filling factors ν_M where M_G jumps. While going from $M_G = 45$ to $M_G = 51 \rightarrow 57$ the pair correlation function develops more pronounced oscillations. We naturally consider this evolution as formation of more rigid solid state order in the system, although the filling factor seems to be too large here to expect WC state in a macroscopic system. If we ignore for the moment what is happening in $M_G = 63$ then the "crystal set" may be smoothly continued to higher momentum states $57 \rightarrow 69 \rightarrow 75 \rightarrow 81 \dots \rightarrow 111$ resulting finally in a quite impressive "long-range" order (see Fig.2). With all the reservations concerning small system size we have to conclude that WC has lower energy than LS in the range of filling factors between $1/3$ and $1/5$.

We also observe a well-defined structure of "satellite states" $|M_G \pm 6n\rangle$ in the energy spectrum for small ν , for example, when $M_G = 81$ we find that $E_{75} - E_G$ and $E_{87} - E_G$ are some five times smaller than the energy of the first

excited state in sectors $M = 75, 81, 87$ (see Fig.3). Note also the remarkable similarity between the low-energy spectra in the basic set of states with $M = M_G \pm 6n$.

Clearly, the state with $M_G = 63$ is special in that its pair correlation function is more "liquid-like" than $g(\theta)$ for both $M_G = 57$ and $M_G = 69$. As mentioned above LS at $\nu = 1/3$ has $M = 63$, thus irregular behaviour of the pair correlation function in this sector may be due to the change of GS from solid to liquid. This suggestion seems to be correct, because the calculated projection of the exact GS for $\nu = 0.32$, i.e., in the middle of the stability interval of the sector $M = 63$ (see Table I), on the Laughlin state is as large as $\langle \Psi_{LS}^{(1/3)} | \Psi_G^{(63)} \rangle = 0.934$, and the ground state energy is extremely well approximated by the variational value $E_{LS}^{(1/3)} = \langle \Psi_{LS}^{(1/3)} | H | \Psi_{LS}^{(1/3)} \rangle$. In Coulomb units we find $E_{LS}^{(1/3)} - E_G^{(63)} = 0.0134$, while the energy of the first excited state in the sector $M_G = 63$ is almost five times higher, $E_1^{(63)} - E_G^{(63)} = 0.0621$. Furthermore, there is no pronounced satellite structure in the low-energy spectrum when $M_G = 63$. Surprisingly enough, the ground state wave function and $g_G(\theta)$ are rather different from $|\Psi_{LS}^{(1/3)}\rangle$ and $g_{LS}(\theta)$. It is clearly seen in Fig.4 that $g_{LS}(\theta)$ is almost flat for large θ and shows no sign of pair correlations across the diameter of our system. These correlations are present in GS. Also, in Fig.5 we plot the average occupation numbers $\langle n(m) \rangle$, calculated in GS and in LS. We see that $\langle n(m) \rangle$ in LS has much smaller amplitude at $m = 0$ and more shallow minimum. As one might expect beforehand, the central particle is not at all localized in the liquid phase.

To clarify the nature of such differences, we construct another variational state, which may be regarded as solid, $|\tilde{\Psi}^{(63)}\rangle$. Consider two nearest solid states, e.g., $|\Psi_G^{(75)}\rangle$ and $|\Psi^{(81)}\rangle$ at some $0.255 < \nu < 0.276$. We notice that their distribution functions $\langle n(m) \rangle$ are very close in shape (see Fig.6), with one particle being localised on orbits with small m (actually $m = 0, 1$; the sum of $\langle n(m) \rangle$ before the minimum is almost 1), and the other six particles occupying extended states with large m . When going from $M_G = 75$ to $M = 81$ the value of $M = \sum_m m \langle n(m) \rangle$ changes by 6 almost entirely due to the change of the occupation numbers of six particles on the first coordination sphere, i.e., $\langle n^{(81)}(m+1) \rangle \approx \langle n^{(75)}(m) \rangle$ for large m . Considering $|\Psi^{(81)}\rangle$ as rotating state with all the pair correlations being preserved, we may construct the variational state $|\tilde{\Psi}^{(75)}\rangle$ close to exact $|\Psi_G^{(75)}\rangle$ according to the rule

$$|\tilde{\Psi}^{(75)}\rangle \sim \sum_{\{m_i\}} C_{\{m_i\}}^{(81)} a_{m_7-1}^\dagger a_{m_6-1}^\dagger \dots a_{m_2-1}^\dagger a_{m_1}^\dagger |0\rangle, \quad (m_{i+1} > m_i), \quad (3.2)$$

where $\sum_i m_i = 81$, and $C_{\{m_i\}}^{(81)}$ are the corresponding exact amplitudes of the expansion $|\Psi^{(81)}\rangle = \sum_{\{m_i\}} C_{\{m_i\}}^{(81)} \prod_i a_{m_i}^\dagger |0\rangle$. Notice that the first particle keeps its states. This procedure is well justified because the first particle is separated from the others by a deep minimum in the distribution function (with $\langle n(m) \rangle$ close to zero in minimum, see Fig.6). To estimate the accuracy of this procedure we project thus obtained variational state on exact $|\Psi_G^{(75)}\rangle$ and find the overlap to be 0.995. We apply now this method to construct $|\tilde{\Psi}^{(63)}\rangle$ from $|\Psi^{(69)}\rangle$ obtained at $\nu = 0.32$, to obtain a solid-state trial wave-function. In Fig.4 and Fig.5 we show the pair correlation function and $\langle n(m) \rangle$ of this state. Finally, the solid-state variational energy turns out to be as good as $E_S^{(63)} - E_G^{(63)} = 0.0075$ and the overlap with GS is $\langle \tilde{\Psi}^{(63)} | \Psi_G^{(63)} \rangle = 0.953$ (even better than that of the Laughlin state!).

From these data we have to conclude that the genuine GS in the range of filling factors $0.294 < \nu < 0.340$ is a mixture of solid and liquid phases with comparable amplitudes. Not only these two quite different states strongly overlap with the ground state and almost minimize the energy, but also $\langle \tilde{\Psi}^{(63)} | \Psi_{LS}^{(1/3)} \rangle = 0.817$. That large overlap is, of course, the finite-size effect. Obviously, under these conditions no definite conclusion about the true GS of the macroscopic system is possible, and there is no contradiction with the experimental fact that at $\nu = 1/3$ the GS is the Laughlin liquid.

We would like to comment here on the widely used argument, based on diagonalization of *finite-size* systems, that large overlap of LS with the exact GS and its precise energy, may serve as a criterion that the corresponding macroscopic system will be an incompressible liquid. We have demonstrated above that this argument simply does not work for the system of seven particles; short-range order in LS and WC turns out to be very similar. One has to analyze more delicate properties (like pair correlation function at large distances) to discriminate between the two phases.

It follows from our data in Fig.2 that GS in the sector $M = 105$ is of solid type. To see how different is $|\Psi_G^{(105)}\rangle$ from $|\Psi_{LS}^{(1/5)}\rangle$ we present in Fig.7 the corresponding correlation functions. We further confirm this result by calculating the overlap between the two states, $\langle \Psi_{LS}^{(1/5)} | \Psi_G^{(105)} \rangle = 0.759$, and the Laughlin state energy $E_{LS}^{(1/5)} - E_G^{(105)} = 0.0188$

(compare with the energy of the first excited state $E_1^{(105)} - E_G^{(105)} = 0.0319$). Now, the admixture of the LS in the structure of GS is much smaller than that at $\nu = 1/3$ and the variational energy is of the order of the first excited state in this sector. To reconcile this result with the experimental observation of the FQHE at $\nu = 1/5$ in some (not all!) systems [7–9], we notice that our result was obtained on finite-size system and for the unscreened Coulomb interaction between the particles. Given rather large difference in energy between LS and WC found in our study, it is likely that WC will be the true GS of a macroscopic system too. This conclusion, however, may change for the screened Coulomb interaction since the Laughlin state is stabilized by short-range interactions. We plan to investigate the role of screening effects on the ground state at $\nu = 1/5$ in a separate paper.

Since the liquid energy is casping down at $\nu = 1/5$, our results give very strong support to the idea that WC exists in the Coulomb system for $\nu > 1/5$. Even if WC is replaced with LS at $\nu = 1/5$ when the interaction potential is screened, it will most likely survive at slightly larger filling factors. We thus conclude that experiments [7–9] did see WC state around $\nu = 1/5$.

IV. OTHER GROUND STATES IN THE PSEUDO-POTENTIAL APPROACH

It was found in Ref. [11] that varying pair potential between the particles in the lowest Landau level one can drastically change the nature of the ground state. In this section we discuss whether this change is of any relevance to Wigner crystallization.

Following Ref. [11] we characterize the potential by the energies, U_m , of pairs of particles with relative angular momentum m . In the lowest Landau level

$$U_m = \int_0^\infty dq q \left(\frac{V(q)}{2\pi} \right) e^{-q^2} L_m(q^2), \quad (4.1)$$

where L_m are the Laguerre polynomials. These are pseudopotential parameters because different bare interactions may have the same values of U_m . For the Coulomb interaction these parameters are $U_m = \sqrt{\pi}(2m-1)!!/(2^{m+1}m!)$ and decrease slowly with m . Spinless fermions are coupled with odd values of m only. The effect of decreasing U_1 for the Coulomb system of $N_e = 6$ electrons on a sphere at $\nu = 1/3$ was the collapse of the Laughlin-type ground state to some gapless state [11] (we will call it U_1 -state). The nature of this state was not clearly identified, although the results did suggest a tendency to charge density wave formation. As we demonstrate below, the gapless ground state obtained by reducing the short-range part of the Coulomb interaction *is not* the conventional Wigner crystal (by "conventional" we mean the single-atom triangular lattice).

We start by noting that the new state has almost zero overlap with LS [11]. This result is in sharp contrast with the large overlap between WC and LS found in Sec. III. This fact alone is sufficient to rule out WC as a candidate for the U_1 -state. Furthermore, as is seen from the data presented in Ref. [11], the collapse of LS *is not* accompanied by formation of the low-energy satellite states corresponding to the rotations of the octahedron formed by six particles on a sphere.

We performed an analogous study of the ground state changes as a function of the U_1 pseudopotential parameter for our system of seven particles. In agreement with Ref. [11] we observe a drastic transformation of the ground state at $\nu = 0.32$ when U_1 is reduced to 0.35. For smaller values of U_1 the ground state angular momentum changes from $M_G = 63$ to $M_G = 56$. The change of M_G by 7, not by 6, also proves that we are not dealing with the conventional WC. Finally, we followed the transformation of the solid ground state with $M_G = 75$ at $\nu = 0.265$ and observed its collapse to the same U_1 -state for $U_1 < 0.32$. These results leave no doubt that reducing the short-range part of the Coulomb potential promotes new ground state other than LS or WC.

To have a better filling about real-space interaction potentials with reduced values of U_1 we show in Fig.8 the particular set of interaction potentials of the form

$$V(r) = \frac{\sqrt{\pi}}{2} e^{-r^2/8} I_o(r^2/8) - \frac{\lambda}{2} e^{-r^2/4}, \quad (4.2)$$

where I_o is the Bessel function. The first term gives the Coulomb interaction between the two unit charges at a distance $r = |r_1 - r_2|$ apart, each being spread out with the Gaussian distribution $(2\pi)^{-1/2} \exp\{-|z - r_i|^2/2\}$, and the second term further suppresses the short-range part of the first. The choice of $V(r)$ in this form is kind of arbitrary. It is justified by the simplicity of its Fourier transform $V(q)/2\pi = (1/q - \lambda) \exp\{-q^2\}$. In a more general case one may also vary the "cutoff length" by letting $r \rightarrow r/r_c$ in the second term. In Fig.8 we plot the potential (4.2) for $\lambda = 0.8, 1.0$, and 1.2 . The corresponding values of U_m are given in Table II. We see that U_1 -state is stabilized at the edge of digging a potential well at short distances.

In Fig.9 we present $\langle n(m) \rangle$ distribution in the U_1 -state with momentum $M_G = 56$. Quite unexpectedly in the U_1 -state, the central particle is replaced with the correlated hole. One has to appreciate this result in the system with the long-ranged Coulomb potential - by taking the central particle from orbits with $m = 0, 1$ and placing it to much higher orbits we substantially increase its mean-field energy. On another hand the "first coordination sphere" of six particles moves to internal orbits thus gaining some mean-field energy. Thus we see, that U_1 -state suggests locally (on the scale of a) inhomogeneous particle distribution. Of course, the long-range tail of the Coulomb potential ensures that the macroscopic system is homogeneous on a large scale $\gg a$, but when the short-range part of the interaction is reduced, the system may choose states with local density higher than average. We are not able to say anything definite about such a state except that it is not conventional WC. Obviously, if the final state is a solid with more than one particle in the unit cell, it can not be traced from the numeric study of seven particles.

V. ACKNOWLEDGEMENT

We are grateful to A.I. Podlivaev for his assistance in writing the exact-diagonalization code. This work was supported by the Russian Foundation for Basic Research (95-02-06191a).

VI. NOTE ADDED

After this work was completed we became aware of the fact that we had overlooked some important experimental results [15] which seem to be in an excellent agreement with our numerical study. In these Refs. a metal - insulator transition is found to occur at the universal filling factor $\nu_c \simeq 0.28$ in rather wide range of magnetic fields and sample mobilities, no reentrant behavior is observed around $\nu = 1/5$. The authors argue that their results could be explained in terms of Wigner crystallization [though other interpretations are not ruled out].

TABLE I. GROUND-STATE ANGULAR MOMENTUM

| GS angular momentum | 21 | 28 | 33 | 39 | 45 | 51 | 57 | 63 | 69 | 75 | 81 | 87 | 93 | 99 | 105 | 111 |
|--------------------------|-------|-------|-------|-------|-------|-------|-------|-------|-------|-------|-------|-------|-------|-------|-------|-------|
| Range of filling factors | | | | | | | | | | | | | | | | |
| ν_{max} | 1 | 0.705 | 0.587 | 0.527 | 0.460 | 0.408 | 0.364 | 0.340 | 0.294 | 0.276 | 0.255 | 0.240 | 0.224 | 0.211 | 0.198 | 0.188 |
| ν_{min} | 0.705 | 0.587 | 0.527 | 0.460 | 0.408 | 0.364 | 0.340 | 0.294 | 0.276 | 0.255 | 0.240 | 0.224 | 0.211 | 0.198 | 0.188 | |

TABLE II. PSEUDOPOTENTIAL PARAMETERS

| Potential | U_1 | U_3 | U_5 |
|-----------------|-------|-------|-------|
| Coulomb | 0.44 | 0.28 | 0.22 |
| $\lambda = 0.8$ | 0.37 | 0.29 | 0.23 |
| $\lambda = 1.0$ | 0.35 | 0.28 | 0.23 |
| $\lambda = 1.2$ | 0.32 | 0.27 | 0.22 |

FIGURE 1.

Pair correlation functions $g(\theta)$ for the ground states in the degeneracy points corresponding to the angular momentum changes $51 \rightarrow 57$, $57 \rightarrow 63$, $63 \rightarrow 69$, and $69 \rightarrow 75$

FIGURE 2.

Pair correlation functions $g(\theta)$ for the ground states at the degeneracy points corresponding to the angular momentum changes $87 \rightarrow 93$, $93 \rightarrow 99$, $99 \rightarrow 105$, and $105 \rightarrow 111$

FIGURE 3.

Low-energy spectrum at $\nu = 0.248$ ($M_G = 81$)

FIGURE 4.

Pair correlation functions $g(\theta)$ at $\nu = 0.32$ for the ground state, the Laughlin state $|\Psi_{LS}^{(1/3)}\rangle$, and the solid state $|\tilde{\Psi}^{(63)}\rangle$

FIGURE 5.

$\langle n(m) \rangle$ distributions at $\nu = 0.32$ for the ground state, the Laughlin state $|\Psi_{LS}^{(1/3)}\rangle$, and the solid state $|\tilde{\Psi}^{(63)}\rangle$

FIGURE 6.

$\langle n(m) \rangle$ distributions for the ground state $|\Psi_G^{(75)}\rangle$ and the excited state $|\Psi^{(81)}\rangle$ at $\nu = 0.265$

FIGURE 7.

Pair correlation functions $g(\theta)$ at $\nu = 0.193$ for the ground state and the Laughlin state $|\Psi_{LS}^{(1/5)}\rangle$

FIGURE 8.

Some realizations of the interaction potential in the real space with reduced values of U_1 .

FIGURE 9.

$\langle n(m) \rangle$ distribution for the U_1 -state at $\nu = 0.32$ and $\lambda = 1.2$.

- [1] R.B. Laughlin, Phys. Rev. Lett., **50**, 1395 (1983).
- [2] J.M. Caillol, D. Levesque, J.J. Weis, and J.P. Hansen, J. Stat. Phys., **28**, 325 (1982).
- [3] See e.g. R.B. Laughlin in *Quantum Hall effect*, eds. R.E. Prange and S.E. Girvin (Springer-Verlag, New York) (1990).
- [4] L. Bonsall and A.A. Maradudin, Phys. Rev., **15 B**, 1959 (1977).
- [5] D.J. Yoshioka and H. Fukuyama, J. Phys. Soc. Japan, **47**, 394 (1979); D.J. Yoshioka and P.A. Lee, Phys. Rev., **27 B**, 4986 (1983). P.K. Lam and S.E. Girvin, Phys. Rev. **30 B**, 473 (1984); *ibid* **31 B**, 613(E) (1985).
- [6] X. Zhu and S.G. Louie, Phys. Rev. Lett., **70**, 335 (1993); R. Price, P.M. Platzman, and S. He, Phys. Rev. Lett., **70**, 339 (1993); P.M. Platzman and R. Price, Phys. Rev. Lett., **70**, 3487 (1993).
- [7] H.W. Jiang, R.L. Willett, H.L. Stormer, D.C. Tsui, L.N. Pfeifer, and K.W. West, Phys. Rev. Lett., **65**, 663 (1990); V.J. Goldman, M. Santos, M. Shayegan, and J.E. Cunningham, Phys. Rev. Lett., **65**, 2189 (1990).
- [8] H.W. Jiang, H.L. Stormer, D.C. Tsui, L.N. Pfeifer, and K.W. West, Phys. Rev., **44 B**, 8107 (1991); H.L. Stormer and R.L. Willett, Phys. Rev. Lett., **68**, 2104 (1992).
- [9] V.J. Goldman, J.K. Wang, and Bo Su, Phys. Rev. Lett., **70**, 647 (1993); T. Sajoto, Y.P. Li, L.W. Engel, D.C. Tsui, and M. Shayegan, Phys. Rev. Lett., **70**, 2321 (1993).
- [10] C. Gros and A.H. MacDonald, Phys. Rev., **42 B**, 9514 (1990).
- [11] F.D.M. Haldane and E.H. Rezayi, Phys. Rev. Lett., **54**, 237 (1985); F.D.M. Haldane in *Quantum Hall effect*, eds. R.E. Prange and S.E. Girvin (Springer-Verlag, New York) (1990).
- [12] V.F. Elesin, V.A. Kashurnikov, L.A. Openov, and A.I. Podlivaev, Physica C 195, 171 (1992).
- [13] V.A. Kashurnikov, A.I. Podlivaev, and B.V. Svidunov, Pis'ma v Z. Eksp. Teor. Fiz. **61**, 375 (1995).
- [14] S. Pissanetzky, *Sparse Matrix Technology*, Academic, Orlando, 1984, ch.6.

[15] S.I.Dorozhkin, A.A.Shashkin, G.V.Kravchenko, V.T.Dolgopolov, R.J.Haug, K. von Klitzing, and K.Ploog, Pis'ma Zh. Eksp. Teor. Fiz. **57**, 55 (1993) [JETP Lett. **57**, 58 (1993)]; S.I.Dorozhkin, R.J.Haug, K. von Klitzing, and K.Ploog, Physica B **184**, 314 (1993); S.I.Dorozhkin, A.A.Shashkin, G.V.Kravchenko, V.T.Dolgopolov, R.J.Haug, K. von Klitzing, and K.Ploog, Izvestia Akademii Nauk (Seria Fizicheskaya), **58**, No.7, 37 (1994) [].

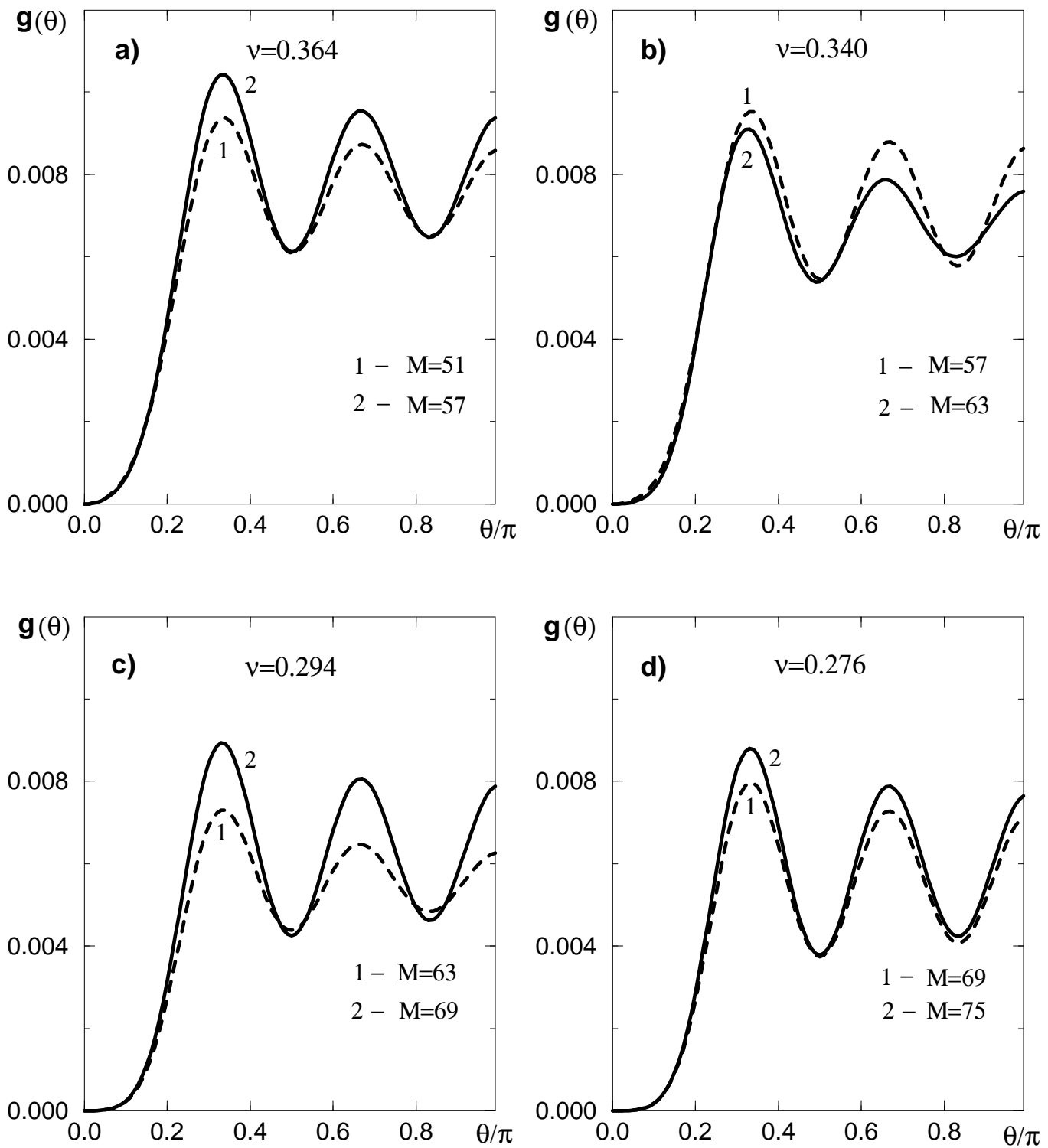


Fig.1

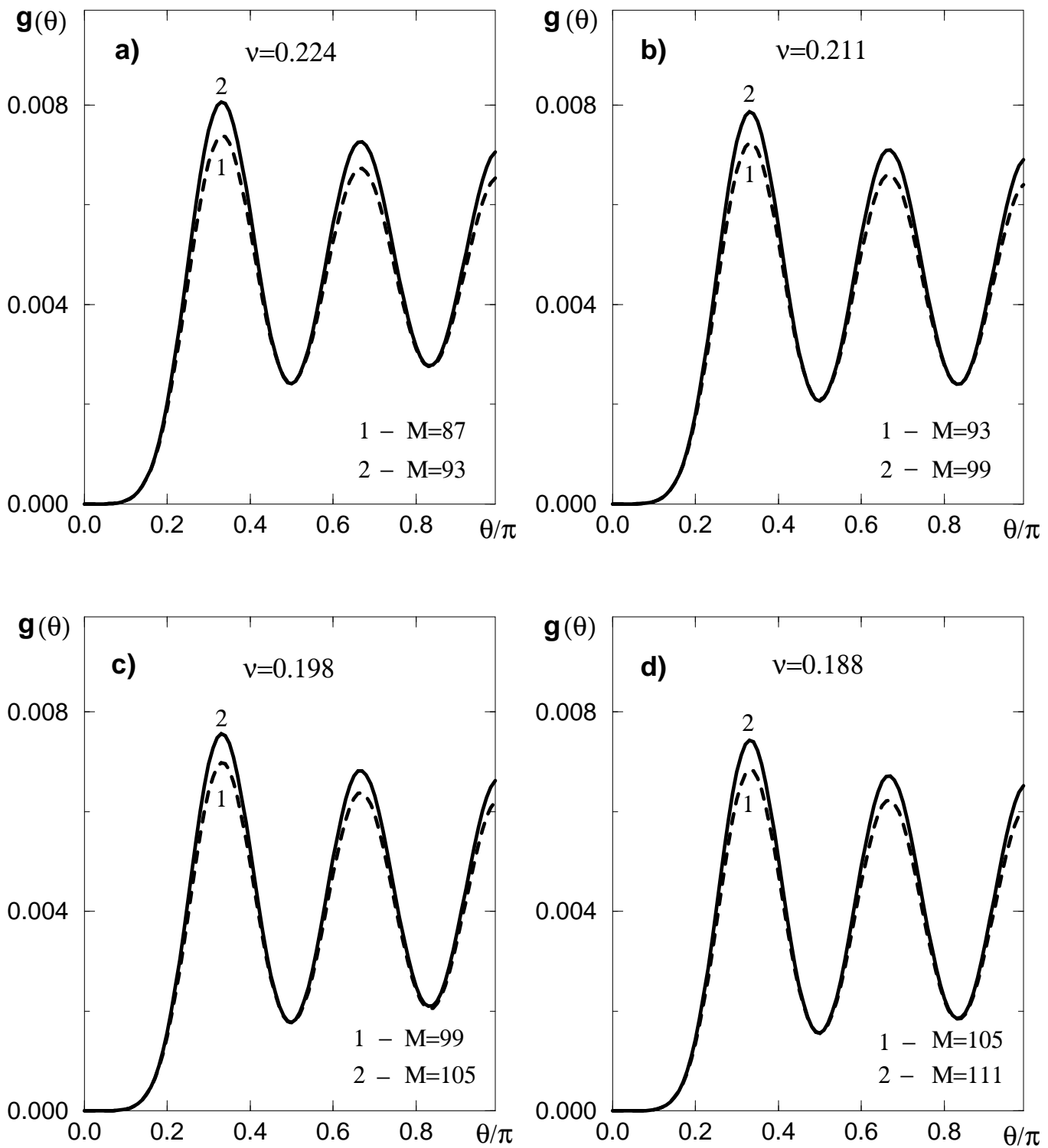


Fig.2

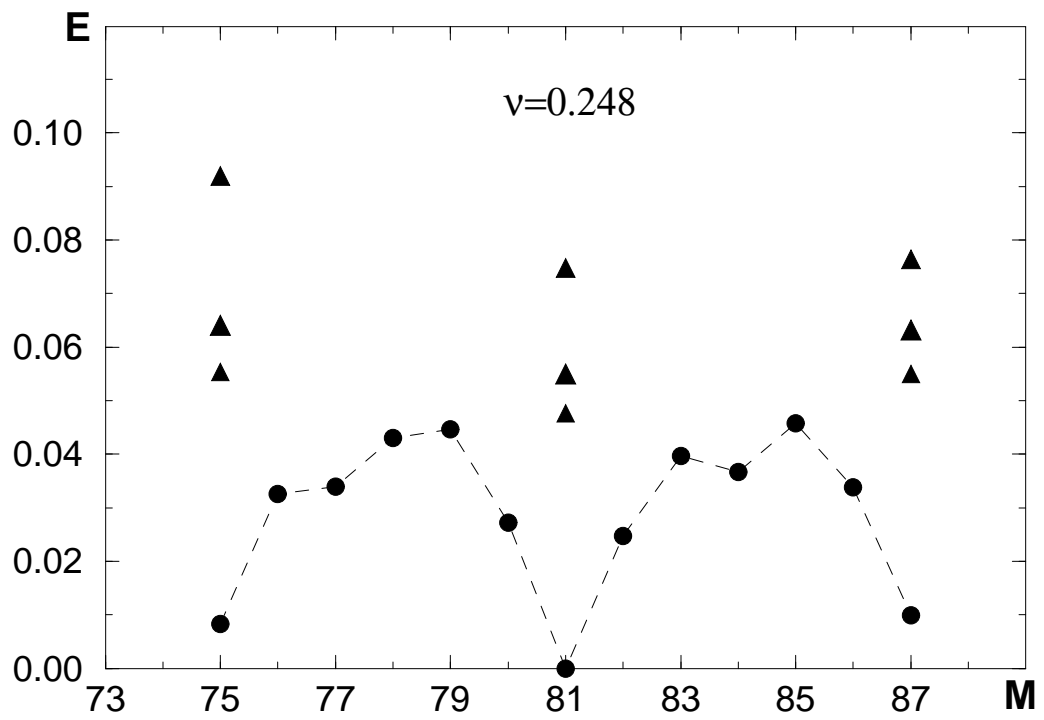


Fig.3

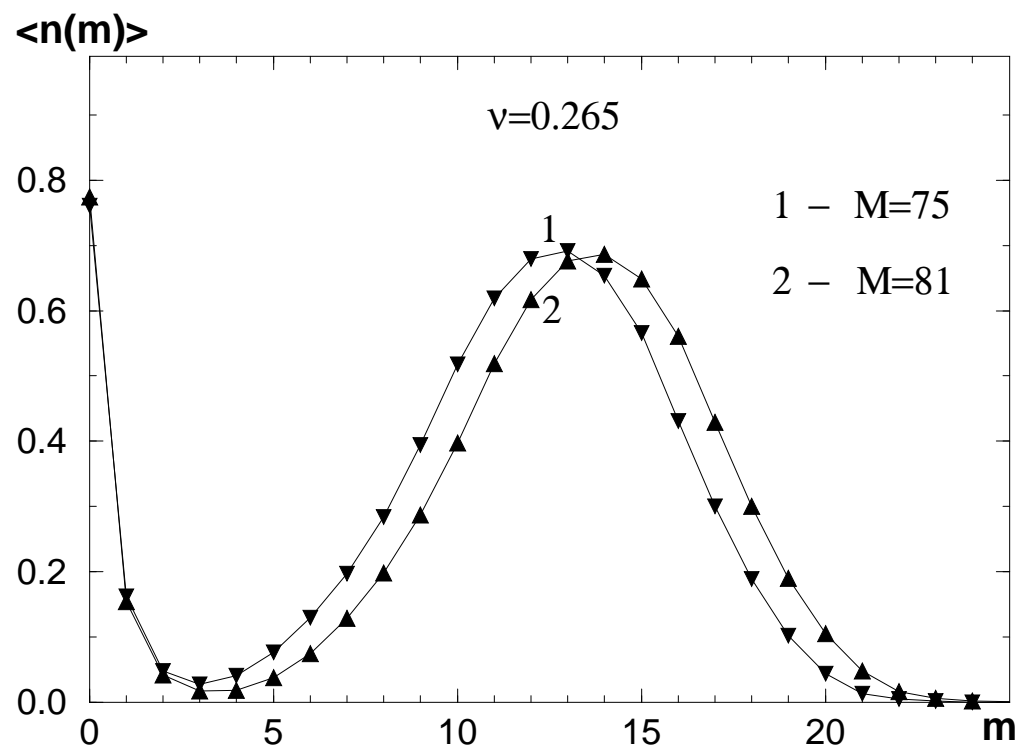


Fig.6

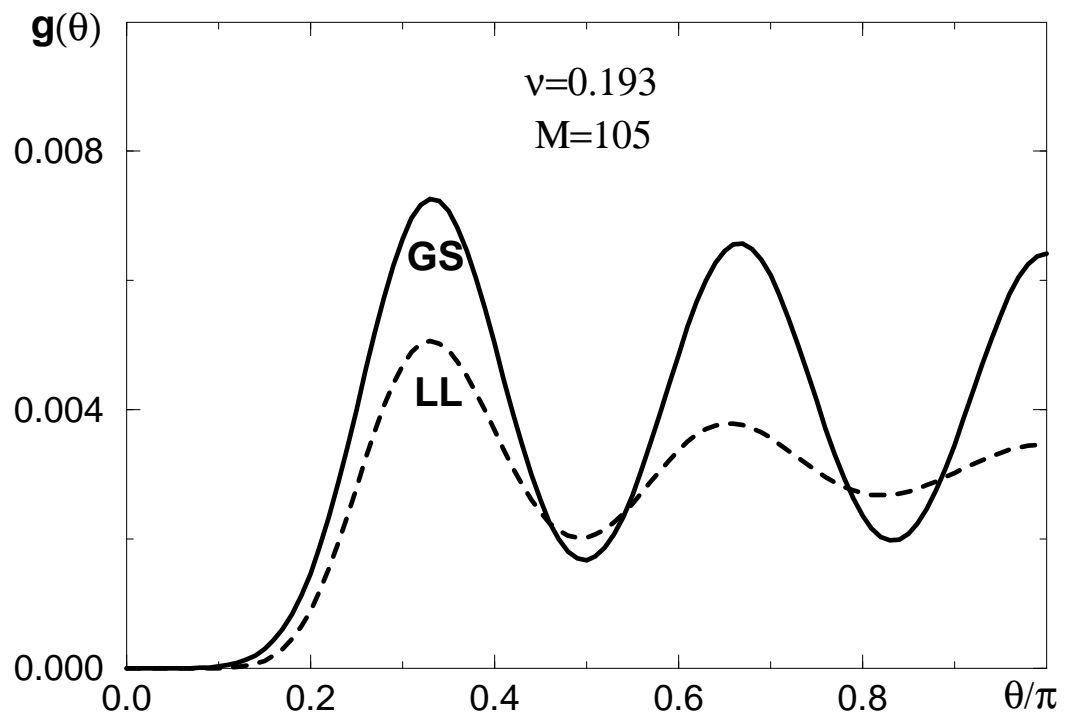


Fig.7

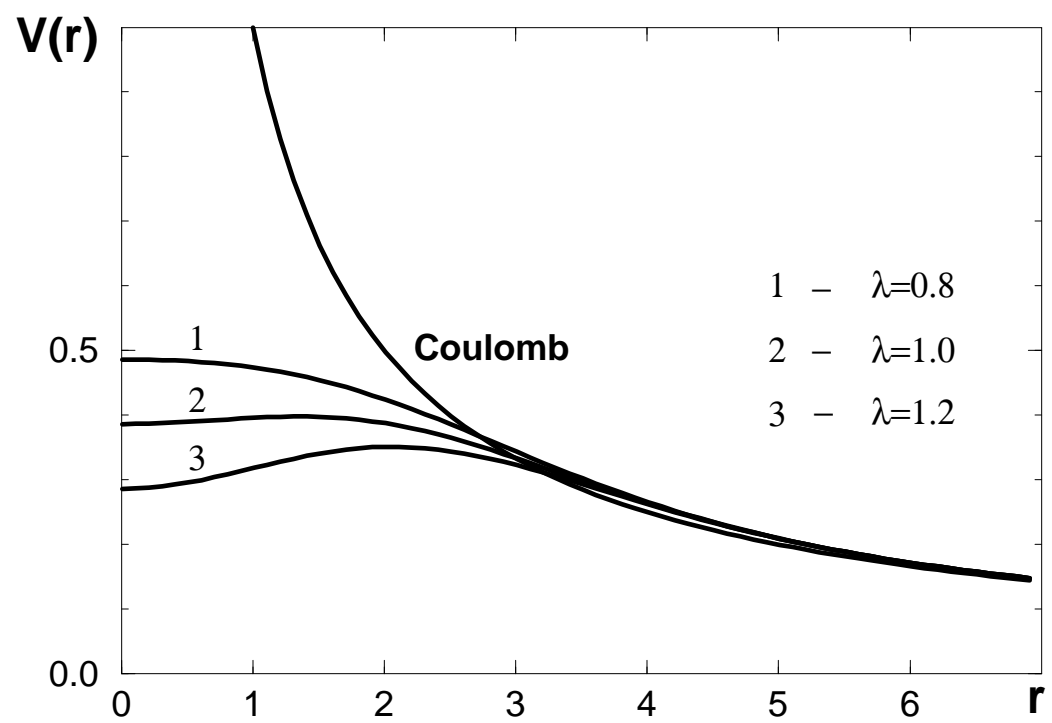


Fig.8

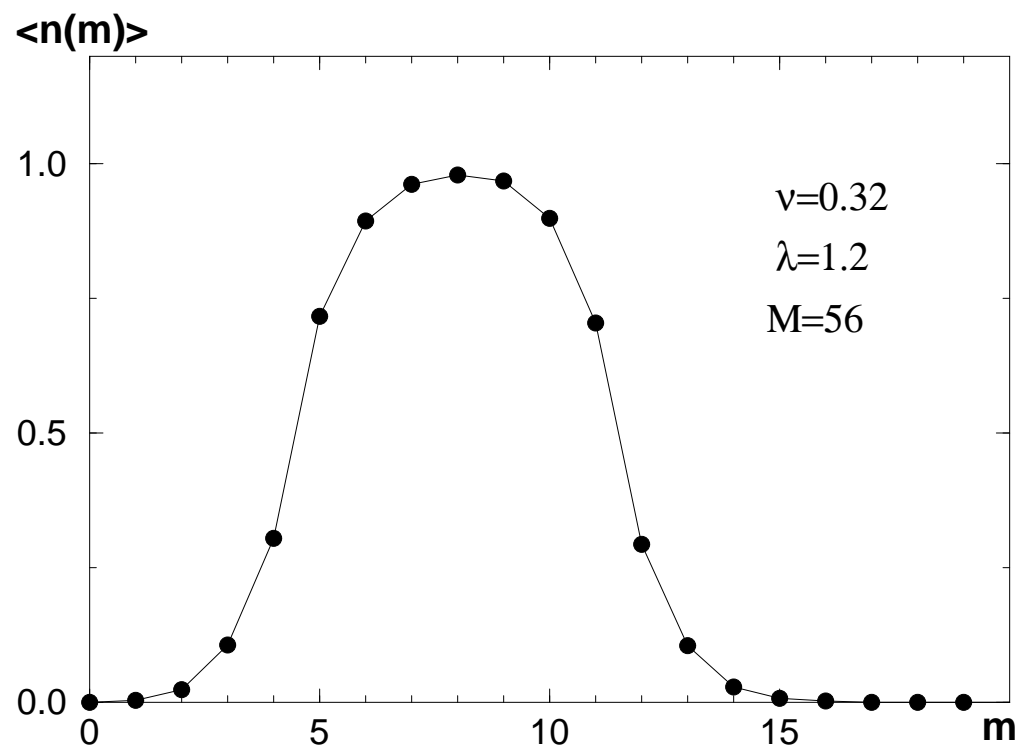
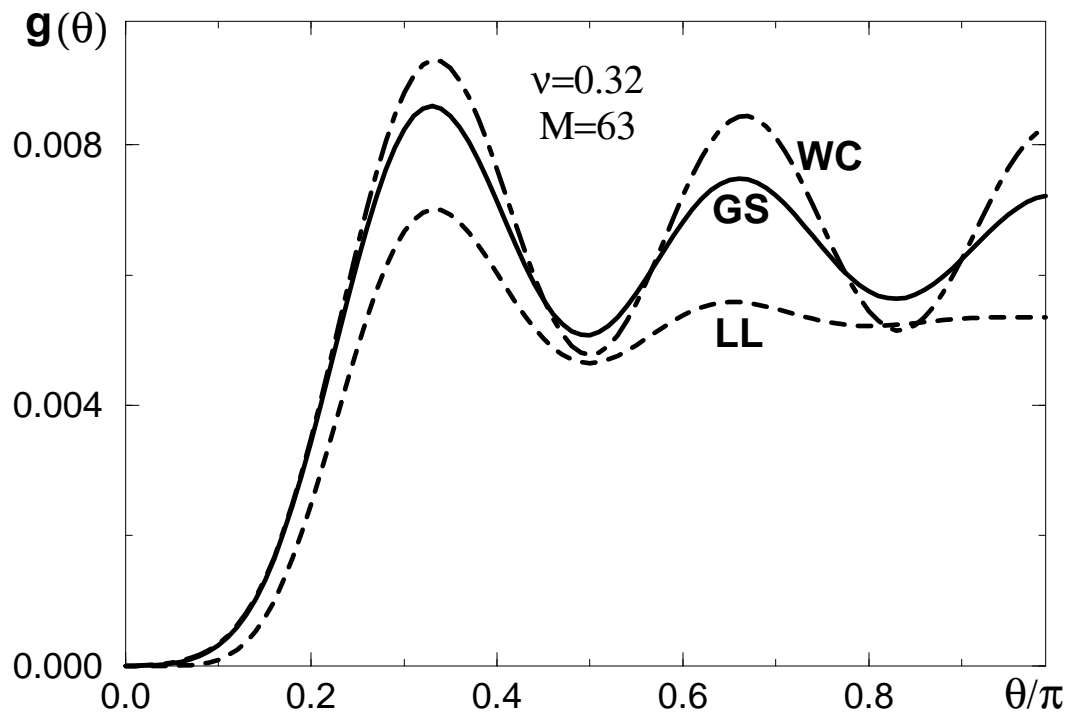


Fig.9



$\langle n(m) \rangle$

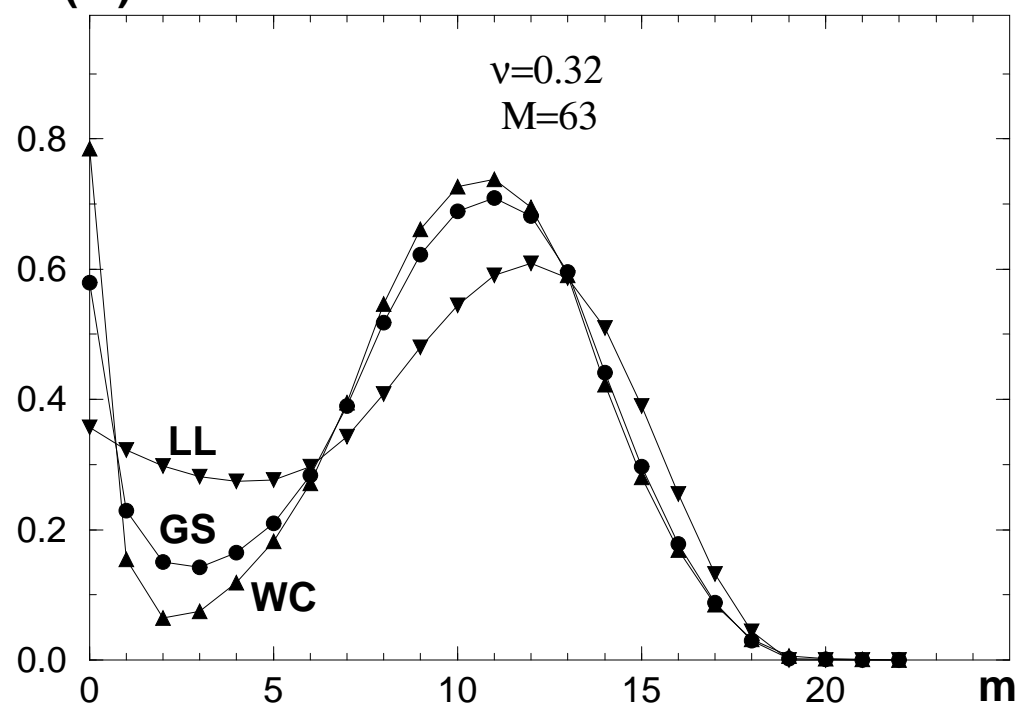


Fig.5